

Charm and prompt photon production with EPOS

This content has been downloaded from IOPscience. Please scroll down to see the full text.

2017 J. Phys.: Conf. Ser. 805 012002

(<http://iopscience.iop.org/1742-6596/805/1/012002>)

View [the table of contents for this issue](#), or go to the [journal homepage](#) for more

Download details:

IP Address: 141.52.96.80

This content was downloaded on 01/08/2017 at 07:51

Please note that [terms and conditions apply](#).

You may also be interested in:

[The impact of the intrinsic charm quark content of the proton on differential \$\gamma + c\$ cross section](#)

S Rostami, A Khorramian and A Aleedaneshvar

[Photon production in heavy ion reactions](#)

Thomas Peitzmann

[Prompt photon hadroproduction at high energies in the kT-factorization approach](#)

A V Lipatov and N P Zotov

[On the possible measurement of gluon asymmetry in a spinning nucleus](#)

M A Yusuf and P Hoodbhoy

[Hard probes and the event generator EPOS](#)

B Guiot and K Werner

[Direct Photon Production in Pion-Proton Collisions](#)

A. I. Ahmadov, C. Aydin and O. Uzun

[QCD: how we can help each other](#)

Jonathan Butterworth

[The effect of neutron skin on inclusive prompt photon production in Pb + Pb collisions at the Large Hadron Collider energies](#)

Somnath De

Charm and prompt photon production with EPOS

B Guiot^{1,2}, Iu Karpenko³, T Pierog⁴, G Sophys² and K Werner²

¹ University Técnica Frederico Santa Maria (UTFSM), Valparaiso, Chile

² SUBATECH, University of Nantes - IN2P3/CNRS - EMN, Nantes, France

³ INFN - Sezione di Firenze, Via G. Sansone 1, I-50019 Sesto Fiorentino (Firenze), Italy

⁴ Karlsruhe Institute of Technology (KIT), IKP, Karlsruhe, Germany

E-mail: benjamin.guiot@usm.cl

Abstract. The implementation of heavy quarks and prompt photons in EPOS is presented. One of the interests of event generators is their capability to reproduce exclusive observables. Our results for charms and prompt photons, in p-p collisions at $\sqrt{s} = 7$ TeV, are compared with experiments and FONLL calculations [1].

1. Introduction

An event generator is an important tool for the understanding of heavy ion collisions because it can be used for realistic studies. With EPOS, one of our goals is the study of the quark-gluon plasma. Several results have already been obtained for light flavors in p-Pb [2, 3] and Pb-Pb [4] collisions. In particular, Epos reproduces the ridge structure and the mass splitting of the elliptical flow coefficients v_2 for pions, kaons, and protons in p-Pb collisions.

Recently, heavy quarks and prompt photons have been implemented in EPOS. These “clean” probes are ideal, for instance, for the study of energy loss in the medium. We plan to study heavy quark correlations in Pb-Pb collisions, which could shed light on energy loss mechanisms [5]. This is a project done in collaboration with J. Aichelin, P.B. Gossiaux, M. Nahrgang and Vitalli Ozvenchuk. Heavy quark propagation in the medium will be studied with the transport code MC@sHQ. Realistic initial conditions for the medium and heavy quark distribution will be provided by EPOS.

EPOS using a unified formalism for p-p, p-A and A-A collisions, heavy quarks and prompt photons have to be implemented only for p-p. After a short presentation of this event generator, we will give some details on hard probes production. Finally, results for D mesons and prompt photons will be shown.

2. EPOS and cut Pomerons

We will not do a general presentation of EPOS which can be found in [3]. I will focus on EPOS multiple interaction (MPI) formalism, in particular on cut Pomerons which are important for inelastic processes. Our formalism, called the parton-based Gribov-Regge theory, is described in very details in [6]. It is based on the Gribov-Regge theory where multiple exchange of Pomerons has been introduced to solve an unitarity issue (see [7] for a short review). In this theory, the



total cross section (related to the elastic cross section by the optical theorem) can be written as

$$\sigma_{tot} = \sum_{m=1}^{\infty} \sigma_m \quad (1)$$

Here, σ_m , the cross section for the diagram with m cut Pomerons, is associated to an inelastic process.

EPOS formalism is based on the same idea. Energy conservation has been added and the nature of Pomerons is not the same since ours include a pQCD part, figure 1.

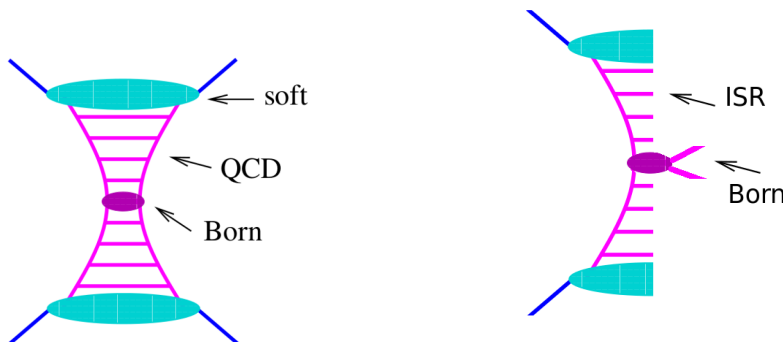


Figure 1. Uncut Pomeron in EPOS.

Figure 2. Cut Pomeron in EPOS. Particle production via initial state radiations (ISR) and the born process.

Diagrammatically, our main formula is shown figure 3 and is a generalization of eq. (1) . Cut

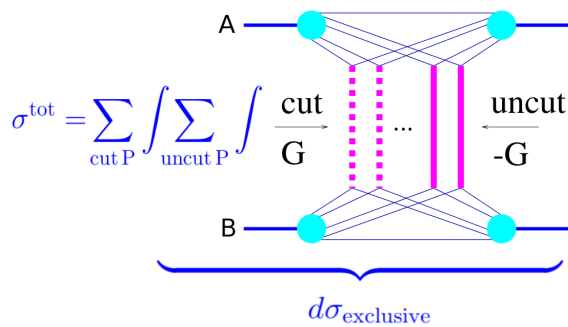


Figure 3. Pink lines : Pomerons. A and B are nuclei. Small horizontal lines are remnants.

Pomerons (figure 2) are central objects for our formalism. First, because they contribute to particle production. In particular, we can write :

$$Multiplicity \propto m \quad (2)$$

$$N_{Dmeson} \propto m \quad (3)$$

m being the number of cut Pomerons. Consequently, we expect a linear rise of the number of D mesons with the multiplicity of charged particles. This has been recently observed by the ALICE collaboration [8] and their results are compared to our simulations figure 4.

Second, because they give initial conditions for the medium. Cut Pomerons are identified as color strings. Regions with a high density of strings will constitute the core, whereas regions

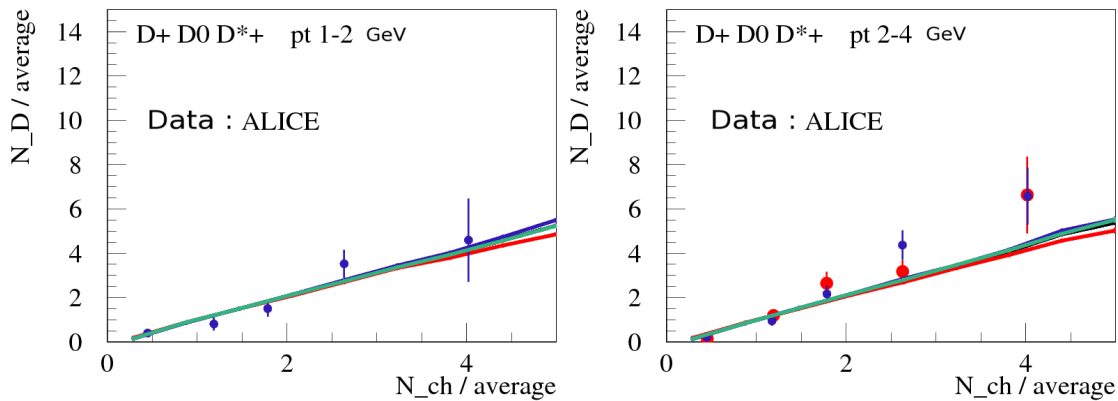


Figure 4. D meson multiplicity as a function of charged particle multiplicity. With EPOS, we obtain a linear rise due to our treatment of multiple interactions. This is in good agreement with ALICE data [8].

with smaller densities will constitute the corona. Quantities like initial energy density for the plasma are provided by cut Pomeron properties. In figure 5 we show the transverse plane with 8 cut Pomerons for one p-Pb collision.

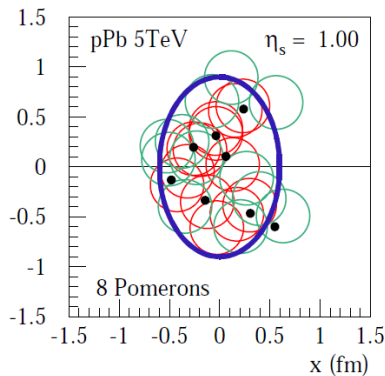


Figure 5. Example of a semi-peripheral p-Pb scattering, with 8 cut Pomerons, showing the transverse plane at space-time rapidity $\eta_s=1$. The positions of the Pomerons are indicated by the black dots. String segment having enough energy to escape (corona) are marked green, the red ones constitute the core. The blue line shows that we obtained an elliptical shape for the core.

In the following, I will present the cut Pomeron building, which includes as a special case hard probes production.

3. Cut Pomeron building and hard probes production

A cut Pomeron is shown 2. The blue line represents a parton coming from the nucleus. If its virtuality is smaller than the saturation scale, $Q^2 < Q_s^2$, it will undergo a soft (non-perturbative) evolution, see [6]. We use the saturation scale to take into account (in a phenomenological way) non linear effects at small x . The usual definition is used :

$$Q_s^2 \sim \frac{A^{1/3}}{x^\lambda} \sim \frac{N_{part}}{x^\lambda} \quad (4)$$

N_{part} being computed at the partonic level (see [3] for more details). When the virtuality becomes bigger than the saturation scale, there is an hard evolution based on DGLAP formalism,

the so-called (spacelike) parton shower (or spacelike cascade). Partons emitted during this cascade are timelike (horizontal pink lines, figure 2) and their transverse momentum is given by :

$$p_t^2 = (1 - \xi)Q^2 - \xi m^2 \quad (5)$$

ξ , the light cone momentum fraction, and m the mass of the timelike parton are shown figure 6.

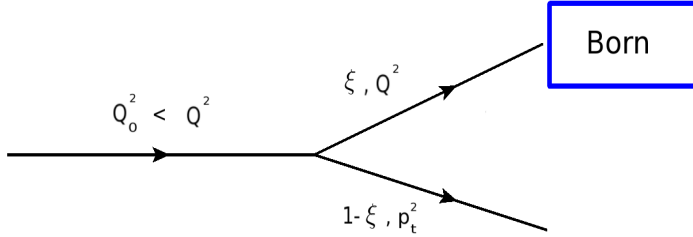


Figure 6. The virtuality, Q^2 , increases after each splitting. Partons emitted during this cascade (initial state radiations), are timelike and carry a light cone momentum fraction $(1 - \xi)$.

During this cascade, hard probes can be produced via the splittings $g \rightarrow c\bar{c}$ and $q \rightarrow q\gamma$.

After the spacelike cascade, the born process is done using leading order pQCD cross sections. The factorization scale is :

$$M_F^2 = \frac{q_t^2}{4} \quad (6)$$

with q_t , the transverse momentum for out born partons. The Monte-Carlo for q_t is based on :

$$\frac{d\sigma_{born}^{ij}}{dq_t^2}(\hat{s}, q_t^2) = \frac{1}{16\pi\hat{s}^2\sqrt{1 - 4q_t^2/\hat{s}}} \sum_{k,l} |M^{ij \rightarrow kl}(\hat{s}, q_t^2)|^2 \quad (7)$$

i and j being the flavor of incoming partons and $|M^{ij \rightarrow kl}(\hat{s}, q_t^2)|^2$ the squared matrix elements. At LHC energies, the dominant process for heavy flavor production is $gg \rightarrow Q\bar{Q}$. Photons are mainly produced by $q(\bar{q})g \rightarrow q(\bar{q})\gamma$ and $q\bar{q} \rightarrow q\gamma$.

Finally, out born partons and those emitted during the hard evolution have a finite virtuality. Each of them (except photons) will initiate a timelike cascade, as shown figure 7. This is the usual Monte-Carlo resummation of soft and collinear divergences. The ordering variable is the virtuality and we use an additional veto for angular ordering. When the decreasing virtuality reaches the lower bound Q_{fin}^2 , the cascade is stopped and hadronization by string fragmentation is performed. Because of our common project MC@sHQ+EPOS, we use :

$$Q_{fin}^2 = m_{charm}^2 = 2.25 \text{ GeV}^2 \quad (8)$$

The initial virtuality for the cascade is :

$$Q_{ini}^2 = p_t^2 + m^2 \quad (9)$$

with p_t^2 defined in eq. (5). As in the spacelike cascade, heavy quarks and prompt photons can be produced via $g \rightarrow Q\bar{Q}$ and $q \rightarrow q\gamma$. The $Q\bar{Q}$ pair is produced at small angle and small transverse momentum. Consequently, the timelike cascade is important for heavy quark distribution at low p_t and heavy quark correlations (gives the pic at $\Delta\phi = 0$).

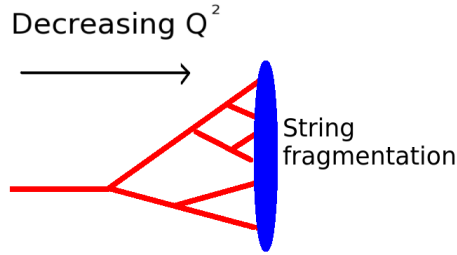


Figure 7. Timelike cascade.

4. Results on charm production

As explained previously, we plan to use charms for the study of energy loss in Pb-Pb collisions. Our charm production has first to be in good agreement with data for p-p collisions. It provides tests for our model, for instance for MPI and parton showers. In figure 8 we show our result for the p_t distribution of charms. A comparison is done with FONLL calculations [1]. p_t distributions

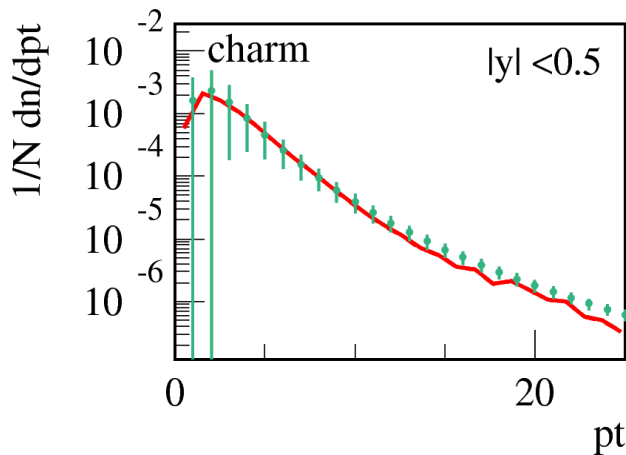


Figure 8. p_t distribution for charms. Green dots are FONLL calculations.

for D mesons are also in good agreement with FONLL calculations and experiments, figures 9 and 10.

Similar results are obtained for D^+ , D_0 and D_s^+ mesons.

5. Isolated photons

Photons can be used for the study of the quark-gluon plasma. For instance, γ /jet events are useful for studies on jet quenching. In this paper, we will study the distribution of the variable x_E :

$$x_E = -\frac{p_t^{asso}}{p_t^{trig}} \cos(\Delta\phi) \quad (10)$$

ideally, p_t^{trig} would be the transverse momentum of a photon produced in the born process. But this is of course a theoretical definition and instead, isolated photons are used in experiments. p_t^{asso} is the transverse momentum of a charged particle in the region $2\pi/3 < \Delta\phi < 4\pi/3$, $0.2\text{GeV} < p_t^{asso} < p_t^{trig}$. $\Delta\phi$ is the azimuthal angle between the photon and its associated particle. The distribution of x_E between 0.2 and 0.9 gives a good approximation of the quark fragmentation function [11]. Comparing distributions of this variable in p-p and Pb-Pb collisions, one can study the modification of the quark fragmentation function by the medium.

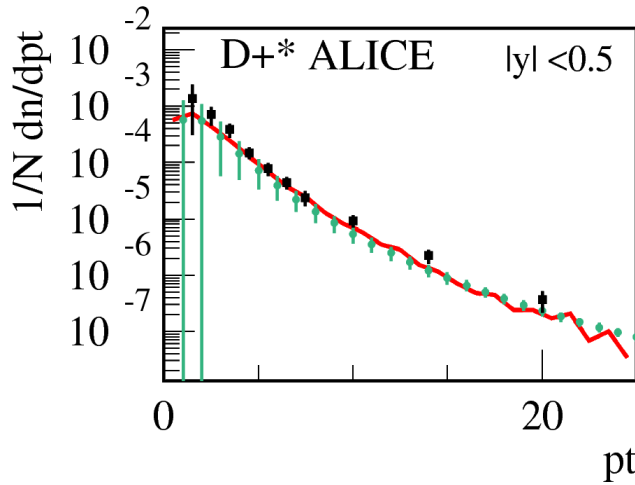


Figure 9. D^{+*} p_t distribution, compared with FONLL calculations (green dots) and ALICE (black squares) [9].

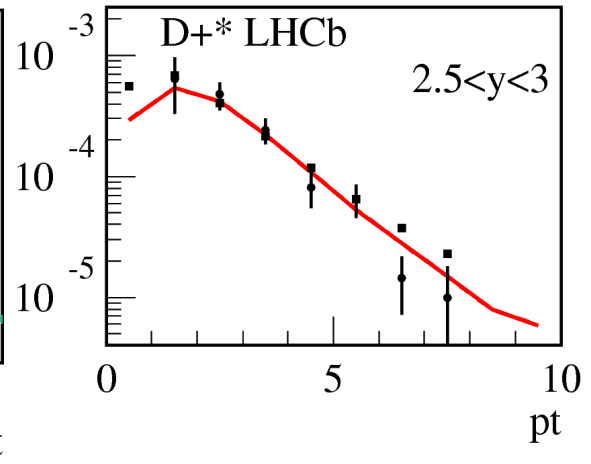


Figure 10. D^{+*} p_t distribution, compared with LHCb (black dots) and Pythia, LHCb tune (black squares) [10].

Recently, fragmentation photons¹ have been implemented in EPOS. Moreover, we use the same isolation criteria as in experiments. Note that this is possible only because, in EPOS, we produce complete events. In each collision, all kind of particles will be produced, even if we are only interested in photons. As expected, fragmentation photons are strongly suppressed by our isolation subroutine, whereas $\sim 98\%$ of direct photons are isolated. Our result for the p_t distribution of isolated photons is shown figure 11 and is in good agreement with CMS measurement [12]. In figure 12 we show the distribution in azimuthal angle of correlations between an isolated

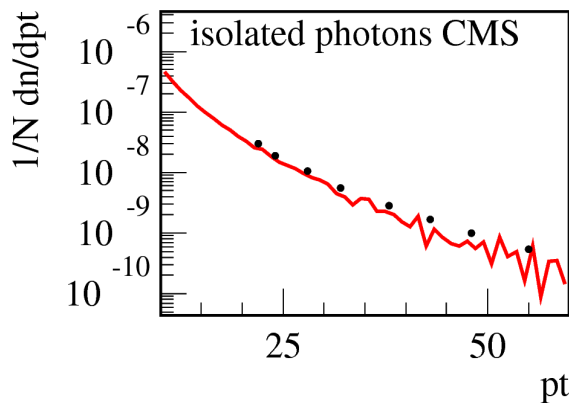


Figure 11. p_t distribution of isolated photons. The comparison is done with CMS [12].

photon and charged particles. By definition, isolated photons are not surrounded by charged particles. This gives the hole (“anti-correlation”) at $\Delta\phi = 0$. The fact that we can reproduce the shape of this plot shows the realistic aspect of EPOS events.

Finally, we show the distribution of the variable x_E figure 13. Our results are in good agreement with experimental data. Here, one can see the interest of event generators which give the

¹ Their are different definitions for fragmentation photons. In this paper, this term is used for photons produced in parton showers.

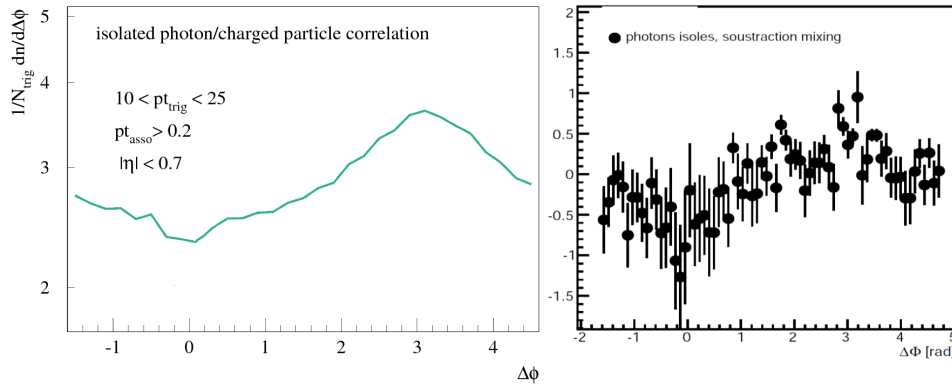


Figure 12. Right : ALICE measurement [13]. Left : EPOS result. The comparison is not done directly with ALICE because we have not performed a mixed event correction. Shapes are comparable, in particular the “anti-correlation” at $\Delta\phi = 0$ is reproduced, showing the realistic implementation of isolation.

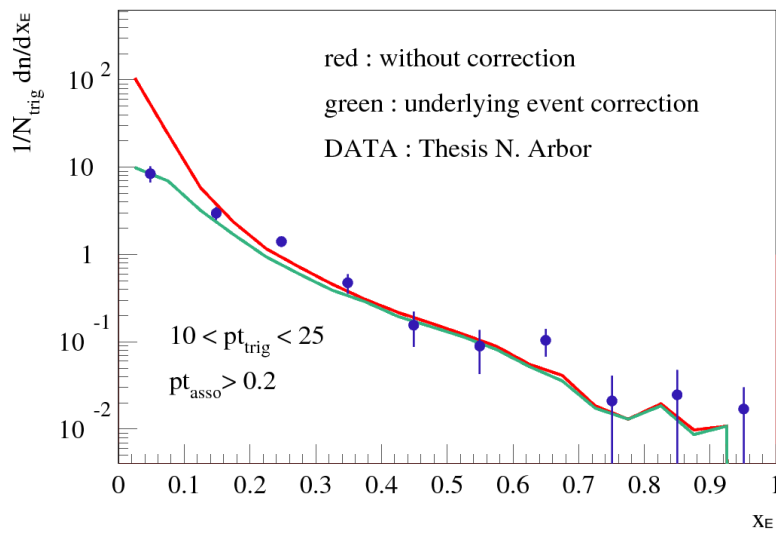


Figure 13. x_E distribution.

possibility to reproduce exclusive observables.

Remark : Fragmentation photons being strongly suppressed by the isolation requirement, these results provide mainly a test for our production of direct photons. Fragmentation photons have still to be tested in more details.

6. Conclusion

Our results for hard probes are in good agreement with experimental data for p-p collisions at 7 TeV. This implementation provides tests for our model, in particular for parton showers. Recently, the bottom quark has also been implemented and some results will be soon published. This event generator shows its good capability to reproduce sophisticated observables like correlations between isolated photons and charged particles and should be a useful tool for the study of the quark-gluon plasma.

Acknowledgement

B Guiot acknowledges the financial support by the TOGETHER project of the Region of “Pays de la Loire“. B Guiot gratefully acknowledges generous support from Chilean FONDECYT grants 3160493.

References

- [1] Cacciari M, Greco M and Nason P 1998 *arXiv hep-ph/9803400*
- [2] Werner K, Bleicher M, Guiot B, Karpenko I and Pierog T 2014 *Phys. Rev. Lett.* **112** 232301
- [3] Werner K, Guiot B, Karpenko I and Pierog T 2014 *Phys. Rev. C* **89** 064903
- [4] Werner K, Karpenko Iu, Bleicher M, Pierog T, Porteboeuf-Houssais S 2012 *Phys. Rev. C* **85** 064907
- [5] Nahrgang M, Aichelin J, Gossiaux P B, Werner K 2013; *arXiv 1310.2218v1*
- [6] Drescher H J, Hladik M, Ostapchenko S, Pierog T and Werner K 2001 *Phys. Rep.* **350** 93
- [7] Werner K 1993 *Phys. Rep.* **232** 87
- [8] Renu Bala, for the ALICE collaboration 2013 *arXiv 1309.6570v1*
- [9] Alice collaboration 2012 *arXiv 1111.1553v2*
- [10] LHCb-CONF-2010-013
- [11] Nicolas Arbor, for the ALICE Collaboration *arXiv 1211.6620v1*
- [12] CMS collaboration 2011 *Phys. Rev. Lett.* **106** 082001
- [13] Nicolas Arbor, thesis 2013